

Water Resources Research®



RESEARCH ARTICLE

10.1029/2022WR034375

Key Points:

- Convolutional Neural Networks applied to satellite images to measure river fragmentation
- More than ten thousand unrecorded barriers identified in Mekong Basin, SE Asia's largest river
- 71.7% of sub-basins in the Mekong Basin are impacted by river barriers, the Chi-Mun Basin is the most fragmented region

Supporting Information:

Supporting Information may be found in the online version of this article.

Correspondence to:

C. Ding and D. He,
chzhding@ynu.edu.cn;
dmhe@ynu.edu.cn

Citation:

Sun, J., Ding, C., Lucas, M. C., Tao, J., Cheng, H., Chen, J., et al. (2024). Convolutional neural networks facilitate river barrier detection and evidence severe habitat fragmentation in the Mekong River biodiversity hotspot. *Water Resources Research*, 60, e2022WR034375. <https://doi.org/10.1029/2022WR034375>

Received 24 DEC 2022

Accepted 19 DEC 2023





Author Contributions:

Conceptualization: Jingrui Sun, Chengzhi Ding, Juan Tao, Xuan Ji
Data curation: Jingrui Sun
Formal analysis: Jingrui Sun, Martyn C. Lucas, Hiuyi Cheng, Jinnan Chen, Mingbo Li, Liuyong Ding, Yan Wang
Funding acquisition: Jingrui Sun, Chengzhi Ding, Daming He
Investigation: Jingrui Sun, Hiuyi Cheng, Jinnan Chen, Mingbo Li, Liuyong Ding, Yan Wang

© 2024. The Authors.

This is an open access article under the terms of the [Creative Commons Attribution-NonCommercial-NoDerivs License](https://creativecommons.org/licenses/by-nc-nd/4.0/), which permits use and distribution in any medium, provided the original work is properly cited, the use is non-commercial and no modifications or adaptations are made.

Convolutional Neural Networks Facilitate River Barrier Detection and Evidence Severe Habitat Fragmentation in the Mekong River Biodiversity Hotspot

Jingrui Sun^{1,2,3} , Chengzhi Ding^{1,2,3} , Martyn C. Lucas⁴ , Juan Tao^{1,2,3}, Hiuyi Cheng⁵, Jinnan Chen^{1,2}, Mingbo Li^{1,2}, Liuyong Ding^{1,2}, Xuan Ji^{1,2}, Yan Wang^{1,2}, and Daming He^{1,2} 

¹Yunnan Key Laboratory of International Rivers and Transboundary Eco-security, Yunnan University, Kunming, China,

²Institute of International Rivers and Eco-security, Yunnan University, Kunming, China, ³Ministry of Education Key Laboratory for Transboundary Eco-Security of Southwest China, Yunnan University, Kunming, China, ⁴Department of Biosciences, University of Durham, Durham, UK, ⁵School of Electronic and Information Engineering, South China University of Technology, Guangzhou, China

Abstract Construction of river infrastructure, such as dams and weirs, is a global issue for ecosystem protection due to the fragmentation of river habitat and hydrological alteration it causes. Accurate river barrier databases, increasingly used to determine river fragmentation for ecologically sensitive management, are challenging to generate. This is especially so in large, poorly mapped basins where only large dams tend to be recorded. The Mekong is one of the world's most biodiverse river basins but, like many large rivers, impacts on habitat fragmentation from river infrastructure are poorly documented. To demonstrate a solution to this, and enable more sensitive basin management, we generated a whole-basin barrier database for the Mekong, by training Convolutional Neural Network (CNN)-based object detection models, the best of which was used to identify 10,561 previously unrecorded barriers. Combining manual revision and merged with the existing barrier database, our new barrier database for the Mekong Basin contains 13,054 barriers. Existing databases for the Lower Mekong documented under ~3% of the barriers recorded by CNN combined with manual checking. The Nam Chi/Nam Mun region, eastern Thailand, is the most fragmented area within the basin, with a median [95% CI] barrier density of 15.53 [0.00–49.30] per 100 km, and Catchment Area-based Fragmentation Index value, calculated in an upstream direction, of 1,178.67 [0.00–6,418.46], due to the construction of dams and sluice gates. The CNN-based object detection framework is effective and potentially can transform our ability to identify river barriers across many large river basins and facilitate ecologically-sensitive management.

1. Introduction

Anthropogenic river barriers including dams, weirs, sluice gates, and bridge aprons alter natural flow regimes, hinder longitudinal connectivity, and alter aquatic habitat (Belletti et al., 2020; Poff et al., 1997; Spinti et al., 2023). These barriers modify river ecosystems directly and indirectly, and can result in substantial biodiversity loss (Grill et al., 2019; Sofi et al., 2020). As one of the persistent threats to freshwater biodiversity, river barrier-derived flow modification and resultant habitat degradation have received great attention globally (Reid et al., 2019; Winemiller et al., 2016). For migratory fishes, river barriers have hindered their migration routes, impeded them from completing their life cycles, and resulted in population declines and local extinctions of many fish species (Lucas & Baras, 2001). For river fish species, barriers isolate gene flow between populations by preventing fish movement between meta-populations, and make them more vulnerable to other anthropogenic stressors and stochastic events (Jones et al., 2021; Radinger et al., 2018).

Historically, research on the environmental effects of anthropogenic river barriers has mainly focused on the impacts of large-scale barriers (e.g., large hydropower facilities and dams) on aquatic ecosystems (Lehner et al., 2011; Vörösmarty et al., 2010). Over two-thirds of large rivers are no longer free-flowing due to the construction of large dams (Grill et al., 2019). More recently concerns have been raised about the negative impacts of small-scale barriers such as weirs, bridge aprons, and sluice gates (Atkinson et al., 2018; Belletti et al., 2020; Sun et al., 2020, 2021). Due to fewer regulations, small-scale river barriers are usually built in greater numbers compared with large-scale barriers (Atkinson et al., 2018; Belletti et al., 2020; Couto et al., 2021), and their cumulative impacts on aquatic ecosystems may be greater (Jones et al., 2021; Lucas et al., 2009). For example, migrating fish may be able to pass a single small barrier, but passage over multiple barriers is

Methodology: Jingrui Sun, Chengzhi Ding, Martyn C. Lucas, Juan Tao, Hiuyi Cheng, Xuan Ji

Project Administration: Jingrui Sun, Chengzhi Ding, Daming He

Resources: Chengzhi Ding

Software: Jingrui Sun, Hiuyi Cheng, Jinnan Chen, Mingbo Li, Liuyong Ding

Supervision: Chengzhi Ding, Daming He

Validation: Jingrui Sun, Hiuyi Cheng, Yan Wang

Visualization: Jingrui Sun

Writing – original draft: Jingrui Sun

Writing – review & editing: Jingrui Sun, Chengzhi Ding, Martyn C. Lucas, Juan Tao, Daming He

increasingly compromised due to cumulative energy consumption, high rates of predation, and other factors (Lucas et al., 2009). Small anthropogenic river barriers have been found to contribute to the decreased abundance of a variety of migratory and non-migratory rheophilic fish species (Birnie-Gauvin et al., 2018; Jones et al., 2021; Sun et al., 2021, 2022).

Several connectivity indices including the Dendritic Connectivity Index (Cote et al., 2009), the Population Connectivity Index (Rodeles et al., 2021), and the Catchment Area-based Fragmentation Index (Jumani et al., 2022) have been developed to assess the impacts of barrier construction on river longitudinal connectivity and to quantify habitat fragmentation. Along with an increased emphasis on measuring river connectivity and habitat fragmentation levels (Jumani et al., 2020; Wohl, 2017), removal or mitigation of the negative impacts of anthropogenic river barriers has become a priority as part of basin-scale restoration planning. River reconnection approaches, including barrier removal and fish pass installation, are now widely employed to restore longitudinal connectivity and fish passage (Silva et al., 2018; Sun et al., 2022). These methods rely on the accuracy and completeness of barrier documentation in existing inventories. A complete barrier inventory can be used to prioritize which barriers to remove or improve connectivity at a basin, depending on modeled benefits, funding availability, and project objectives (King et al., 2017). Across the globe, several river barrier databases are publicly available. Most of these databases were built for large barriers, and small barriers are normally poorly documented (but see North American Great Lakes Barrier Database, Januchowski-Hartley et al., 2013; Adaptive Management of Barriers in European Rivers (AMBER) Barrier Atlas, Belletti et al., 2020; Global River Obstruction Database (GROD), Yang et al., 2022). In order to enable effective river restoration, it is necessary to understand the true numbers, distribution, and types of barriers across entire basins. To do this, most, and ideally all, barriers within the basin need to be mapped and categorized, to generate a proper barrier inventory (Atkinson et al., 2018; Belletti et al., 2020; Januchowski-Hartley et al., 2013).

Several barrier detection methods have been developed to identify and locate river barriers. Traditional methods include walkover surveys (Jones et al., 2019; Sun et al., 2020), which require the river network to be surveyed by fieldworkers, which is time-consuming and labor-intensive. About 10 km of river channel can be walkover-surveyed per person per day (Sun et al., 2020). Visual interpretations of remotely sensed photographic images (Atkinson et al., 2018; Yang et al., 2022) are effective but also time-consuming (approximately 80~100 km of river can be surveyed per person per day depending on the number of river barriers and complexity of the surveyed river reach; Sun, Du, et al., 2023), making it difficult to conduct across large areas. Other methods include manual or automated (e.g., machine learning) interpretation of high-resolution remotely sensed data derived from Light Detection and Ranging (LIDAR) or Synthetic Aperture Radar (SAR) (Buchanan et al., 2022; Entec, 2010). These enable more rapid acquisition of barrier location data, but require costly access to equipment to obtain DEM data or high-resolution images. An additional approach identifies intersections of the river network with transport crossings to identify potential barriers (Januchowski-Hartley et al., 2013), but may require further steps to check the validity of each potential barrier. The scarcity of accurate and relatively complete basin-scale barrier inventories, other than for just the largest dams, is a major impediment to river conservation in many parts of the world.

In recent years, with the rapid development of deep learning algorithms, convolutional neural networks (CNNs) have been widely employed for object detection from remotely sensed images (Liu et al., 2019). This approach has been successfully used to identify reservoirs and large dams from satellite images, by extracting deeper image features through CNNs (Fang et al., 2019, 2021; Jing et al., 2021), making it possible to apply to river barrier detection across large-scale areas. However, river barriers comprise several different types and a variety of sizes (Belletti et al., 2020) which, when associated with variations in environmental background and weather conditions, could increase the object diversity, reducing detection of barrier “objects” (Saeed et al., 2021). No previous attempts have been made using CNNs to detect small-scale barriers or multiple barrier types such as weirs and sluice gates across a large-scale river basin.

In this study, we propose a new river barrier detection framework that is able to identify different river infrastructures within satellite images. The framework was applied to multiple object detection models with an associated manual revision step. A custom global river barrier satellite image database covering both flow-impounding structures and flow-regulating structures was built and used to train selected CNN models. Flow-impounding structures classically include dams (hydropower facilities or reservoir dams, with impounded areas clearly evident immediately upstream), but also sluices, which impound water over variable time scales for flood and tide water management (Garcia de Leaniz & O’Hanley, 2022). Flow-regulating structures are typically weirs

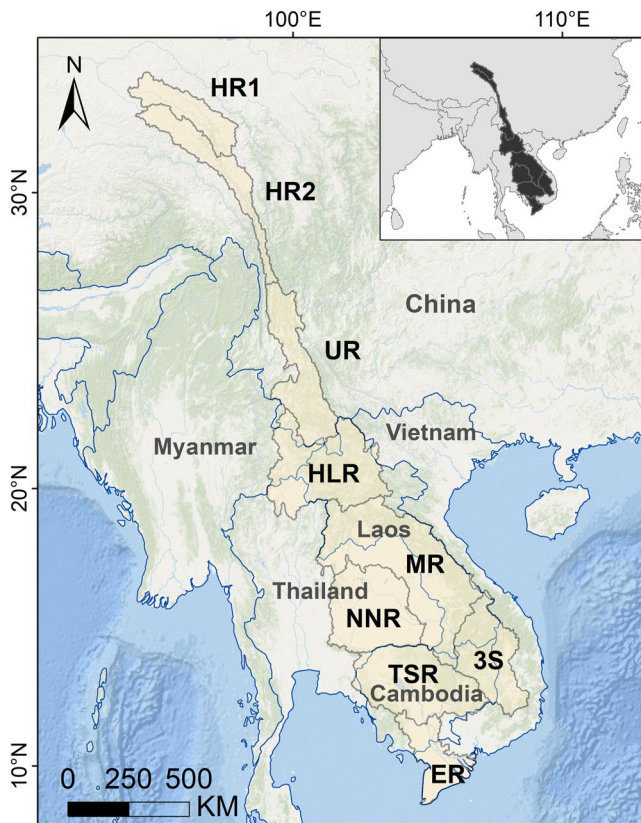


Figure 1. The Mekong Basin, six surrounding countries, and nine biogeographical regions for freshwater fish species in the basin: Headwater Region 1 (HR1), Headwater Region 2 (HR2), Upper Region (UR), Highland Region (HLR), Middle Region (MR), Nam Chi and Nam Mun Region (NNR), Sekong, Sesan, and Srepok Region (3S), Tonle Sap Region (TSR), Estuary Region (ER).

(run-of-river flow-regulating structures, in which water normally overflows the crest of the structure), but also include structures such as bridge aprons (Garcia de Leaniz & O’Hanley, 2022). The best-performing CNN model was retained and applied to identify barriers across a large scale. In this case, the Mekong Basin, one of the world’s freshwater biodiversity hotspots in Southeast Asia (Kang & Huang, 2021; Tao, Ding, et al., 2023; Winemiller et al., 2016), was used as our study site, in order to identify previously unrecorded river barriers. Internationally, there is a focus of debate on the impacts of current and planned proliferation of river infrastructure throughout the Mekong Basin (Sun, Galib, et al., 2023; Winemiller et al., 2016; Ziv et al., 2012). Although previous studies suggest existing barrier databases are highly incomplete for the Mekong Basin (Baumgartner et al., 2022; Sun, Du, et al., 2023), no thorough, publicly-open, basin-scale, barrier database currently exists (Sun, Galib, et al., 2023). Therefore, the distribution of river barriers within the Mekong Basin, and their impacts on river habitat fragmentation, were re-assessed using our newly created barrier database.

2. Materials and Methods

2.1. Study Area

The Mekong River, the largest transboundary river in East and Southeast Asia, originates in China and flows through Myanmar, Thailand, Laos, Cambodia, and Vietnam (Figure 1). The basin covers an area of approximately 805,809 km², and mainstream length (Strahler stream order ≥ 6) is 7,928 km. To facilitate data analysis, interpretation, and management options, the Mekong Basin was first categorized into nine regions (i.e., Headwater Region One (HR1), Headwater Region Two (HR2), Upper Region (UR), Highland Region (HLR), Middle Region (MR), Nam Chi and Nam Mun Region (NNR), Sekong, Sesan and Srepok Region (3S), Tonle Sap Region (TSR), Estuary Region (ER)) based on the biogeographical regions of freshwater fish species in the basin (Kang & Huang, 2021). Then, a total of 1,130 sub-basins (Hydrobasin level 8) were identified according to the HydroBASINS spatial layer within the HydroSHEDS database (<https://www.hydrosheds.org/>).

2.2. River Barrier Image Training Set Development

A river barrier satellite image dataset (Google Earth GEOTIF images, 1 m resolution, shot between year 2020 and 2021) containing a variety of river infrastructure types spanning the globe, was generated to train the barrier detection candidate models. To maximize the capability of the model for detecting different types of river barriers, barriers of different shapes, sizes, and functions were needed. To do that, three existing barrier datasets, namely the GROD database (Yang et al., 2022), AMBER Barrier Atlas (Belletti et al., 2020), and the Lancang River Barrier Database (LRBD) (Sun, Du, et al., 2023) were used (see in Supporting Information S1). Large hydropower facility and reservoir dam data were mainly extracted from the GROD database, and small river barriers such as small dams, weirs, bridge aprons, and sluice gates were mainly extracted from the AMBER and Lancang barrier databases. The numbers of barriers derived from each database used for CNN training, validation and testing are displayed in Table S1 in Supporting Information S1, while their geographical distribution is shown in Figure S1 in Supporting Information S1.

To collect satellite images of anthropogenic river barriers, a total of 10,000 barrier coordinates including latitude and longitude were randomly selected from these datasets. A 680 × 680 pixels square polygon (appropriate size that could cover the majority of river barriers within a single image at 1 m resolution) was built for each coordinate, using the R packages “rgdal” and “rgeos” (Bivand et al., 2021, 2022), and saved as a shapefile with the package “sf” (Pebesma et al., 2022). Shapefiles were imported in Bigemap GIS office, to download the

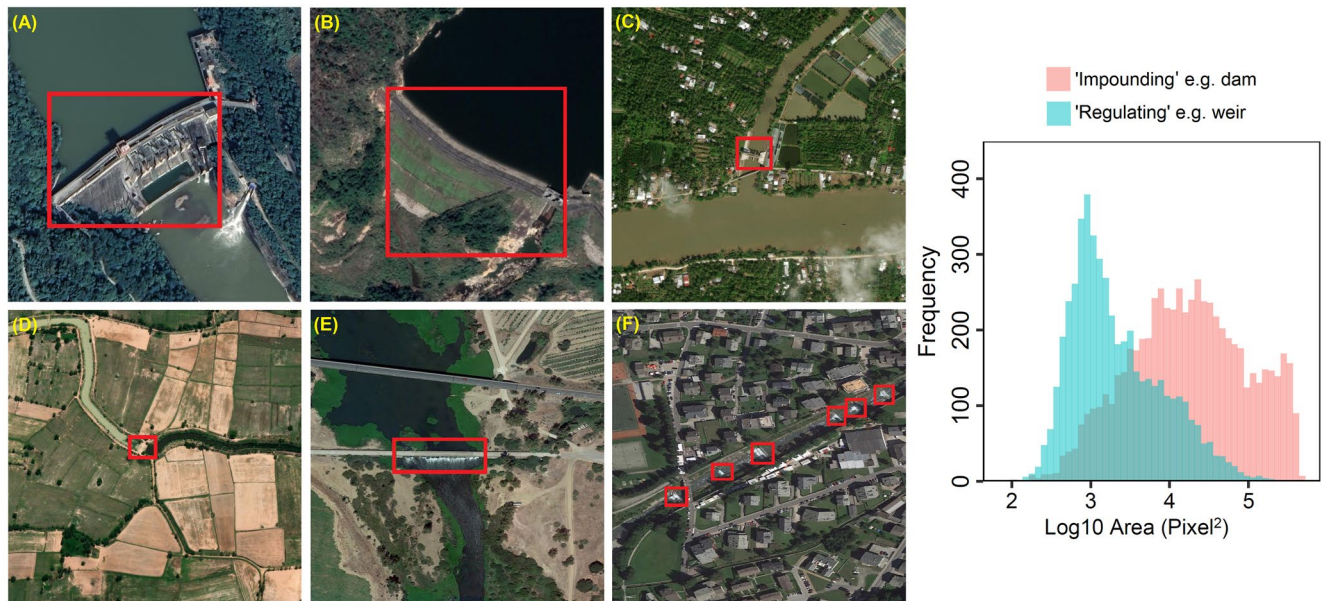


Figure 2. Example types and sizes of barriers from satellite images used for training and validation using convolutional neural network models. Left panel, examples of labeled river barriers, “Impounding” type barriers: (a) large hydropower facility, (b) large reservoir dam, (c) sluice gate, (d) small earth dam; “Flow-regulating” type barriers: (e) bridge apron, (f) weirs. Right panel, area (pixel²) of two types of river barrier used in training and validation data. Note the log x scale.

corresponding Google Earth GEOTIF images. Each image was manually checked, images with no barriers or barriers shaded by overlapping trees were deleted, and duplicated barriers were removed. After that, a total of 8,246 images were retained for further processing.

The open-source image labeling software LabelMe (Russell et al., 2008) was used to mark barriers within each image. For each barrier, a rectangular bounding box was manually created to fully surround the structure (Figure 2). For barriers with complex shapes, an appropriate polygon was used to label the barrier. When an image contained multiple barriers, each barrier was framed with a different bounding box. During the labeling process, all barriers were categorized into two main types: Impounding structures (including large hydropower facilities, reservoir dams, and sluice gates) and flow-regulating structures including weirs and bridge aprons, based on their physical features (Garcia de Leaniz & O’Hanley, 2022). A total of 6,375 Impounding-type barriers and 4,886 Regulating-type barriers were labeled. The areas of detection boxes ranged from 70 to 454,251 pixel², with a median [quartiles] area of 17,535 [5,096–61,588] pixel² for Impounding-type barriers and 1,548 [784–5,153] pixel² for regulating-type barriers (Figure 2). Due to large variations in barrier sizes, small-scale barriers like weirs may only have a few pixels in an image, which increases the difficulty of detection. To increase the size of both the object and bounding box, the tailwater (white-colored water located immediately downstream of the structure) of the small-scale structure (i.e., weir and bridge apron) was also framed with the barrier. After labeling, all bounding box data were saved in COCO format JSON files (Lin et al., 2014).

2.3. Baseline Models and Experimental Settings

Before training, all images and associated corresponding JSON files were randomly divided into training, validation, and test sets with a ratio of 8:1:1 (Jing et al., 2021; Moortgat et al., 2022; Segal-Rozenhaimer et al., 2020). A total of 6,596 images with 9,014 detection boxes were categorized as the training set, 825 images with 1,169 detection boxes were categorized as the validation set, and 825 images with 1,078 detection boxes were categorized as the test set (Figure S1 and Table S1 in Supporting Information S1). Several object detection-based models were used to identify and locate river barriers within each image. Anchor-based multi-stage methods including faster regions with convolutional neural networks (Faster R-CNN, Ren et al., 2015), Cascade Mask R-CNN (Cai & Vasconcelos, 2019), Libra-Faster R-CNN (Pang et al., 2019), and anchor-free one-stage methods, Fully Convolutional One Stage (FCOS, Tian et al., 2019) and Foveabox (Kong et al., 2020), were used to evaluate their performance on the river barrier satellite dataset. Detailed information of selected models and their architectures are available in Supporting Information S1.

Table 1
Comparison of the Performance of Various Object Detection Models on the Barrier Test Data Set, at the Intersection Over Union (IoU) Threshold of 0.5

Method	Backbone	Recall	AP ₅₀	APweir	APdam
Faster-RCNN	Resnet-50	0.848	0.656	0.629	0.684
	Resnet-101	0.828	0.635	0.623	0.648
	ResNext-101	0.838	0.663	0.636	0.689
Cascade-Mask-RCNN	Resnet-50	0.836	0.625	0.617	0.633
	Resnet-101	0.838	0.650	0.652	0.648
	ResNext-101	0.862	0.609	0.637	0.582
Libra-Faster-RCNN	Resnet-50	0.849	0.619	0.605	0.633
	Resnet-101	0.835	0.635	0.615	0.655
	ResNext-101	0.852	0.649	0.640	0.659
FCOS	Resnet-50	0.927	0.688	0.662	0.715
	Resnet-101	0.934	0.677	0.687	0.666
	ResNext-101	0.935	0.704	0.698	0.711
Foveabox	Resnet-50	0.915	0.656	0.646	0.666
	Resnet-101	0.903	0.672	0.646	0.698

Note. The best recall value is shown in bold. AP₅₀ (mean average precision over an IoU of 0.5) is a common metric for assessing the efficacy of models for object detection.

The open-source MMDetection framework (Chen et al., 2019) was used for implementing the above methods in our benchmark dataset. The pre-trained backbones including ResNet50, ResNet101, and ResNext101 were applied for training different models. Each model was trained under its standard default implementation with adaptive improvements. A total of 24 epochs were trained for each model, where the slope of the loss curve turned flat indicating that the model was well trained (Figure S2 in Supporting Information S1). Then, each epoch was validated with the validation dataset. As the main objective of the study was to discover as many unrecorded river barriers as possible, to maximize the barrier retrieval rate, we selected the best performance model based on highest recall with relatively highest precision (Figure S2 in Supporting Information S1). Average precision metrics were also calculated for all barriers and impounding (dam) and regulating (weir) types. The specific details of the methods and backbones used for training are given in Table 1, and a detailed explanation of each evaluation metric can be found in Supporting Information S1. Omission and commission errors of each barrier detection method were compared with the test set (Figures S3 and S4 in Supporting Information S1). Overall, the FCOS achieved less confusion with other objects, and missed fewer river barriers (Figures S3 and S4 in Supporting Information S1). Taken together, we kept the FCOS ResNext-101-FPN as the best-performing barrier detection model (with a recall of 0.935 at an Intersection over Union [IoU] threshold of 0.5; see Table 1) in the MMDetection framework. The network architecture of the FCOS model is shown in Figure 3 (Tian et al., 2019; see in Supporting Information S1 for detailed explanation).

2.4. Application Method for Large-Scale River Barrier Detection

The Lower Mekong Basin (for the purposes of this study, downstream of the UR region; Figure 1) was chosen for applying the CNN barrier detection method. Due to its large basin area, it is not possible to input the entire satellite image of the basin into the MMDetection framework for barrier detection. In addition, satellite images without river features (i.e., those without river channels and related aquatic features) contain too much background information, which could reduce the calculation efficiency and occupy a large amount of hard drive storage. In order to solve this problem, only images with river features (river channels, lakes with afferent and efferent channels etc.) were selected for barrier detection. To download the satellite images (Google Earth images generated

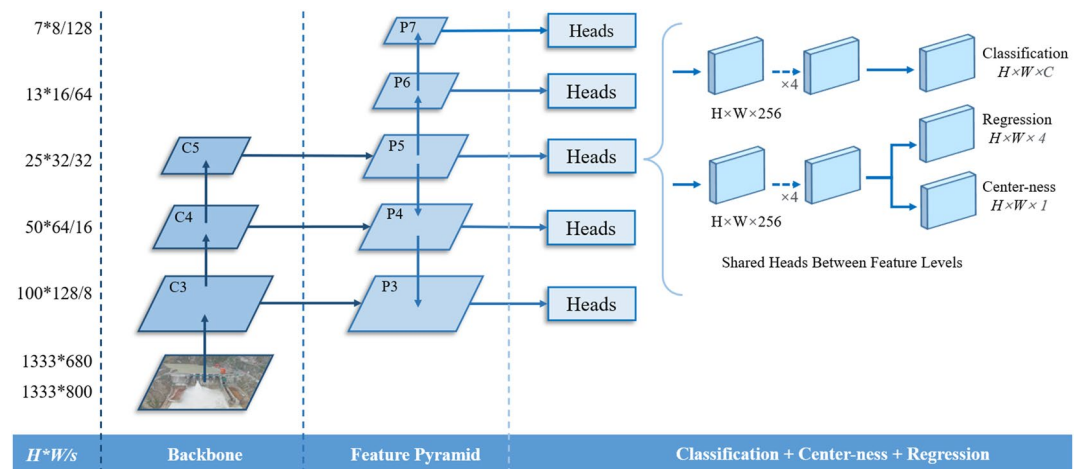


Figure 3. The network architecture of the Fully Convolutional One Stage model. $H \times W$ represent the height and width of feature maps. C3 to C5 denote the feature maps of the backbone network. P3 to P7 are the feature levels used for the final prediction.

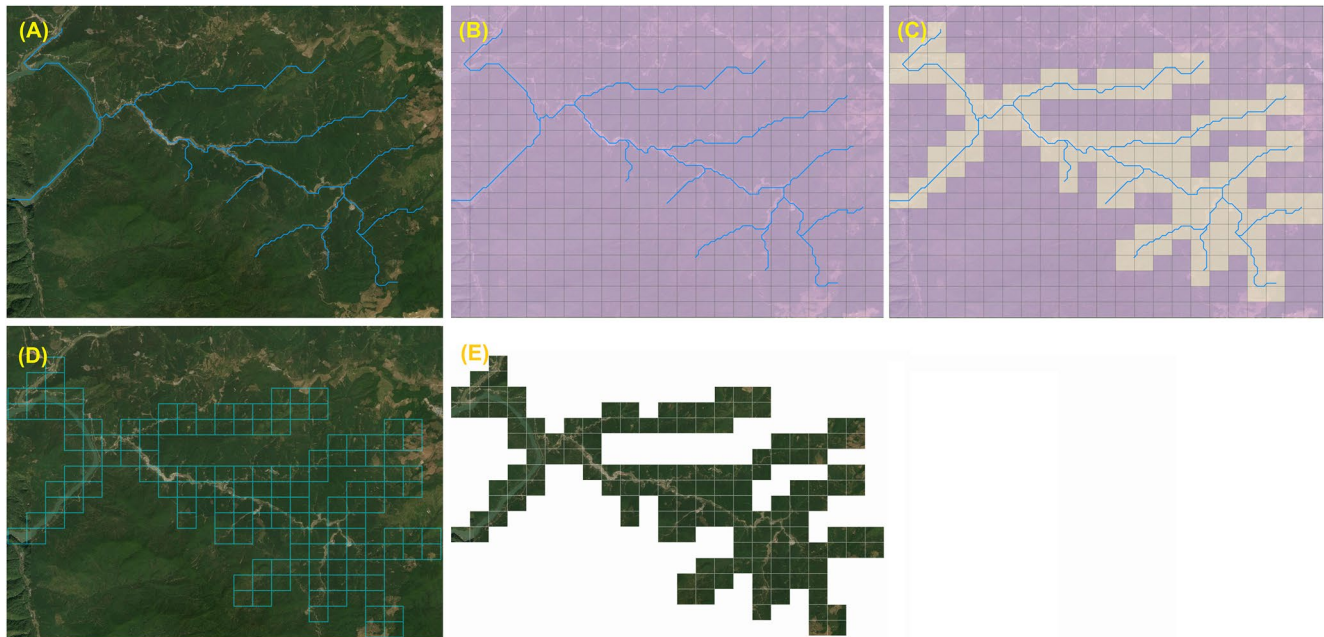


Figure 4. The river satellite images downloading process: (a) an example sub-basin and river network polyline, (b) fishnet matrix (filled with 680×680 pixels cells/polygons) created covering the whole area, (c) selected polygons that were proximate to the river network, (d) retained polygons based on the river network, (e) downloaded river network satellite images based on polygons.

in 2020–2021) for river network areas only, a 90 m resolution basin-scale river network (i.e., polylines) (Wang et al., 2021) was used to locate all river segments. Then, a large matrix filled with 680×680 pixel cells (polygons) was created at 1 m resolution, covering the whole lower Mekong Basin area (Figure 4, panel B). The “select by location” function of ArcGIS was used to select cells that were proximate to the river network (Figure 4, panel C), and all selected cells were saved as shapefiles (Figure 4, panel D). Figure 4 demonstrates how this process was performed, using a small sub-basin to showcase the process.

For the Mekong delta region (ER in Figure 1), due to intensive development in canals and dike systems, the natural river channels have been largely altered (Hung et al., 2012), so river network polylines are unable to match the actual channels in satellite images. In this case, all cells in the Mekong delta region were saved as shapefiles rather than selected as river networks. Overall, the lower Mekong Basin was split into a total of 1.4 million cells. After that, all shapefiles were imported into Bigemap GIS office, to download the corresponding Google Earth satellite images (shot between year 2020 and 2021) at the same resolution scale (1 m).

All images were tested with our best-performing barrier detection model (FCOS ResNext-101-FPN) in the MMDetection framework. Bounding boxes of potential river barriers with a score threshold exceeding 0.3 were retained, and drawn on corresponding images. After that, the coordinates (latitude and longitude) of the midpoint of each bounding box were extracted from the corresponding GEOTIF image, using the “GDAL” package (Rouault et al., 2021) in Python. Then, each image with potential barriers were manually checked by at least two members from the pre-trained team, via Microsoft Excel Visual Basic function (Figure S5 in Supporting Information S1). During this step, potential barriers and their coordinates were loaded in an Excel file, then each detected object was judged by clicking “Yes” (= anthropogenic river barrier), “No” (not an anthropogenic river barrier) or “Not sure” buttons on the panel. The confirmed barrier was visually categorized by type (i.e., dam, weir, sluice gate, bridge apron, and others; Figure 5), by clicking the corresponding button (Figure S5 in Supporting Information S1). Objects classified as “Not sure” were re-assessed by another researcher before a final decision. To resolve commission errors, during this step, misidentified objects (e.g., bridges, river banks, rice field ridges, and farms) were removed from the river barrier list (Figure 6). If undetected river barriers (barriers without bounding boxes) were found on the image, then they were manually recorded, as a compensation approach to reduce omission errors. The country, sub-basin identity (level 8), and altitude (m above sea level) in which it was located were recorded, and a unique ID code was assigned, to form the Lower Mekong River Barrier Database (LMBD).

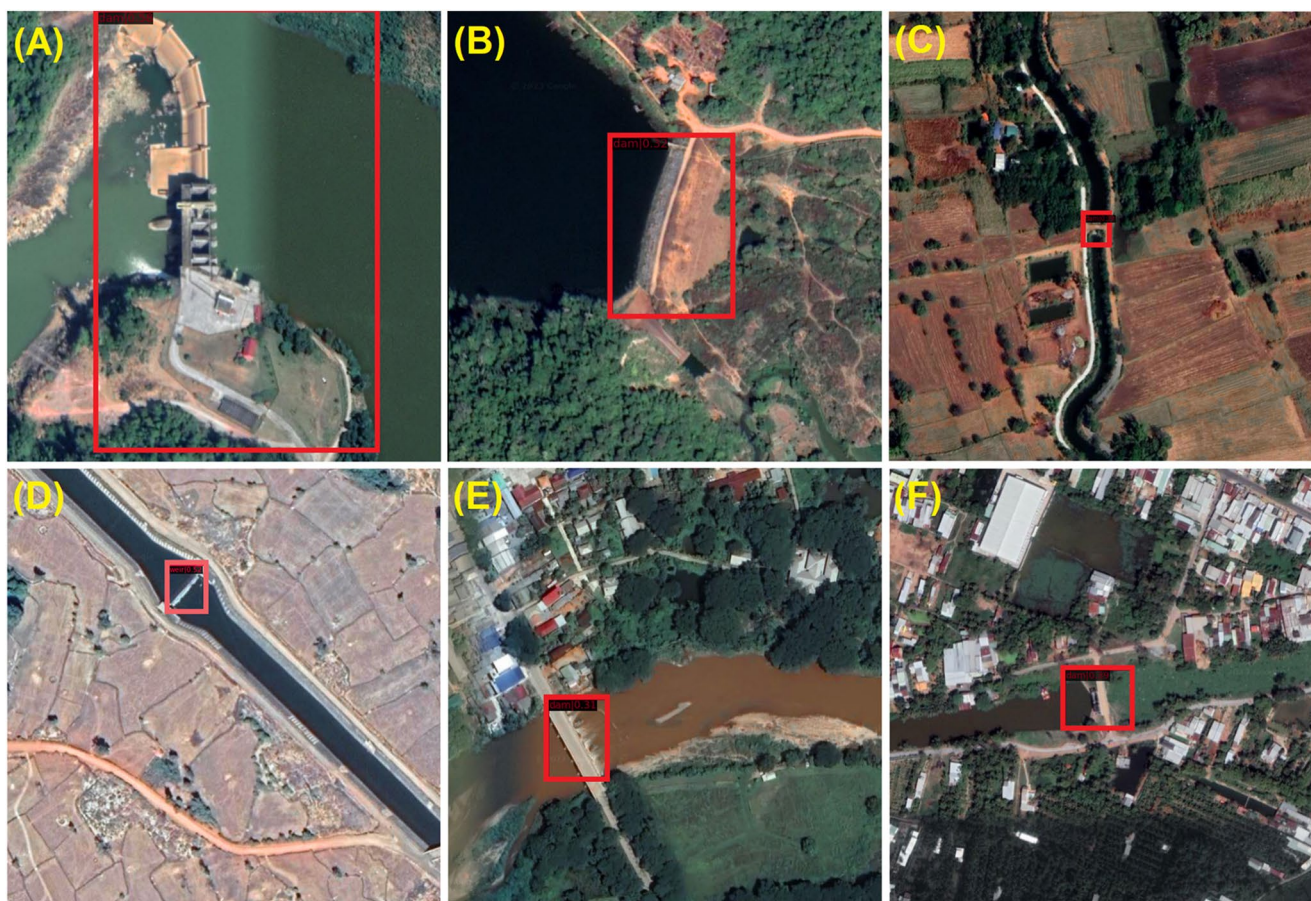


Figure 5. Examples of objects identified river barriers by the Fully Convolutional One Stage model in the Mekong Basin. (a) large hydropower facility, (b) large reservoir dam, (c) small earth dam, (d) weir, (e) bridge apron, (f) sluice gate.

Barriers coordinates from both the LMBD and the Lancang River Barrier Database (LRBD, comprising HR1, HR2 and UR regions) were then added to ArcGIS to remove duplicates (within a distance of 50 meters) using the ‘Near’ tool. Then a complete Mekong River Barrier Database (MRBD) was formed.

2.5. Model Enhancement

Due to the geographic specificity in the lower Mekong Basin, it was observed that certain “barrier-like” objects were misidentified as river barriers by the initial FCOS model. To mitigate the commission errors, and enhance the model performance, an additional 1,897 images (all containing genuine barriers, coordinates extracted from the MRBD database) from 16 sub-basins of the Mekong Basin were incorporated to the original training/validation/test sets, to enable further training the FCOS model.

To compare the performance of the initial and enhanced FCOS models in the Mekong Basin, a total of 20 sub-basins (Hydrobasin Level 8; different from the aforementioned 16 sub-basins) from the Lower Mekong were randomly selected, for conducting searches of satellite images to identify river barriers. Then, the accuracy of both FCOS models were calculated and compared. Accuracy was calculated as $(\text{true positives} + \text{true negatives}) / (\text{true positives} + \text{true negatives} + \text{false positives} + \text{false negatives})$ and expressed as a percentage.

2.6. Comparison Against Existing Barrier Database

Existing river barrier data for the Mekong Basin were collected from two open access databases: Global River Obstructions Database (GROD) (Yang et al., 2022), and the Greater Mekong Subregion Hydropower Dams (GMSHD) Database (Barbarossa et al., 2020; Open Development Mekong, 2016). Prior to our study, these were

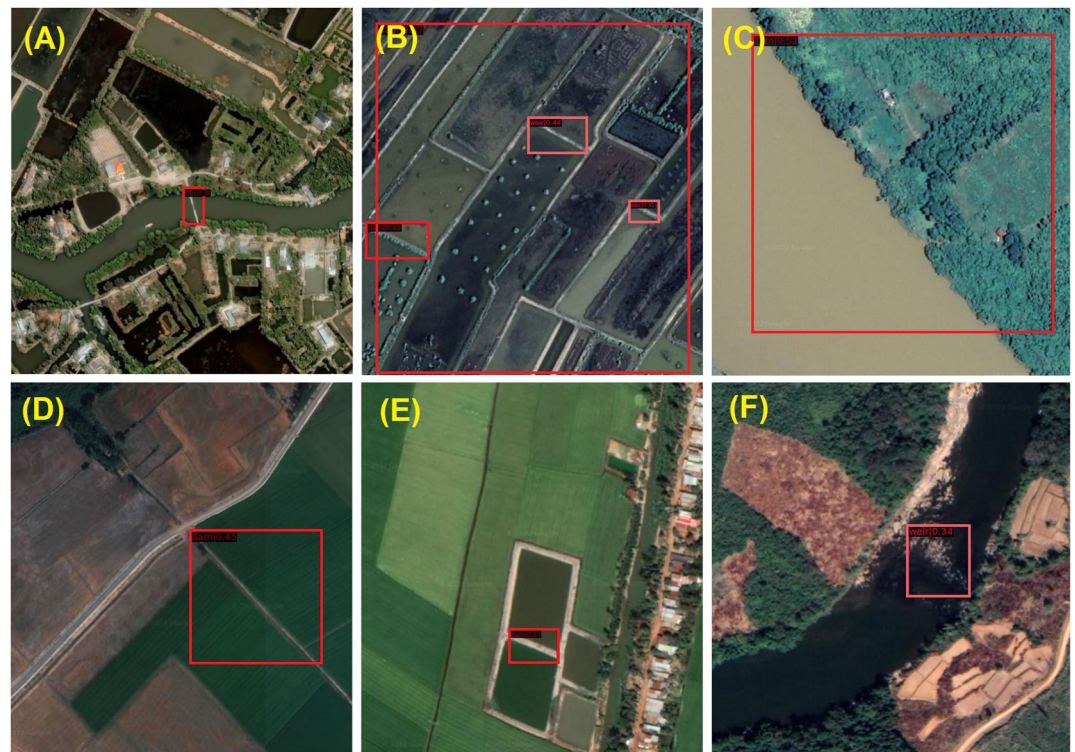


Figure 6. Examples of objects misidentified as anthropogenic river barriers by the Fully Convolutional One Stage model. (a) small bridge without bridge apron, (b) rice field ridges, (c) river bank, (d) farm edge, (e) fish pond, (f) natural bedrock.

the two most up-to-date barrier databases covering the Mekong region, suitable for comparison against. Only existing barriers and barriers that were under construction were recorded, planned dams/hydropower facilities were excluded from further analysis. Barrier density was used as a measure of regional river fragmentation (Jones et al., 2019; Sun, Du, et al., 2023). For each sub-basin, the river length was calculated according to the HydroRIVERS database. Barrier density was calculated for each sub-basin, using the total number of barriers divided by the total river length within the given sub-basin. Barrier densities from the three databases, GROD, GMSHD and MRBD were calculated separately.

2.7. Fragmentation Assessment of the Mekong Basin

To evaluate the impacts of river barriers on aquatic habitat, the Catchment Area-based Fragmentation Index (CAFI) (Jumani et al., 2022) was calculated for each sub-basin (Figure 7). The CAFI (Equation 1) is calculated based on the basin area, the number, location, and impassability of barriers within a given sub-basin (Jumani et al., 2022). In this study, dams and heavily modified channels (categorized within “Others” in the database, but mainly comprising sections of channel converted to linked rice paddies and bunded ponds; Figure S6 in Supporting Information S1) were assumed to be impassable due to their physical dimensions and form, so an impassability of 1 was given (Baumgartner et al., 2022; Grill et al., 2014). For partially permeable barriers including weirs, bridge aprons, and sluice gates, three impassability values (high: 0.8, moderate: 0.5, low: 0.2) were assigned in order to explore the effect of impassability on CAFI outputs within the basin (Shaad et al., 2018).

$$CAFI = \sum_{i=1}^n \frac{a_i \times c_i}{A} \quad (1)$$

where, “n” is the number of river barriers within the specific sub-basin; “ a_i ” is the total sub-basin area of barrier “i”; “ c_i ” is the barrier impassability score ranging from 1 (impassable) to 0 (completely passable); “A” is the basin area of the entire river network.

CAFI values were calculated from two directions: from downstream to upstream, and from upstream to downstream (Jumani et al., 2022). Values of CAFI were calculated using the R packages “terra” and “sf” (Hijmans

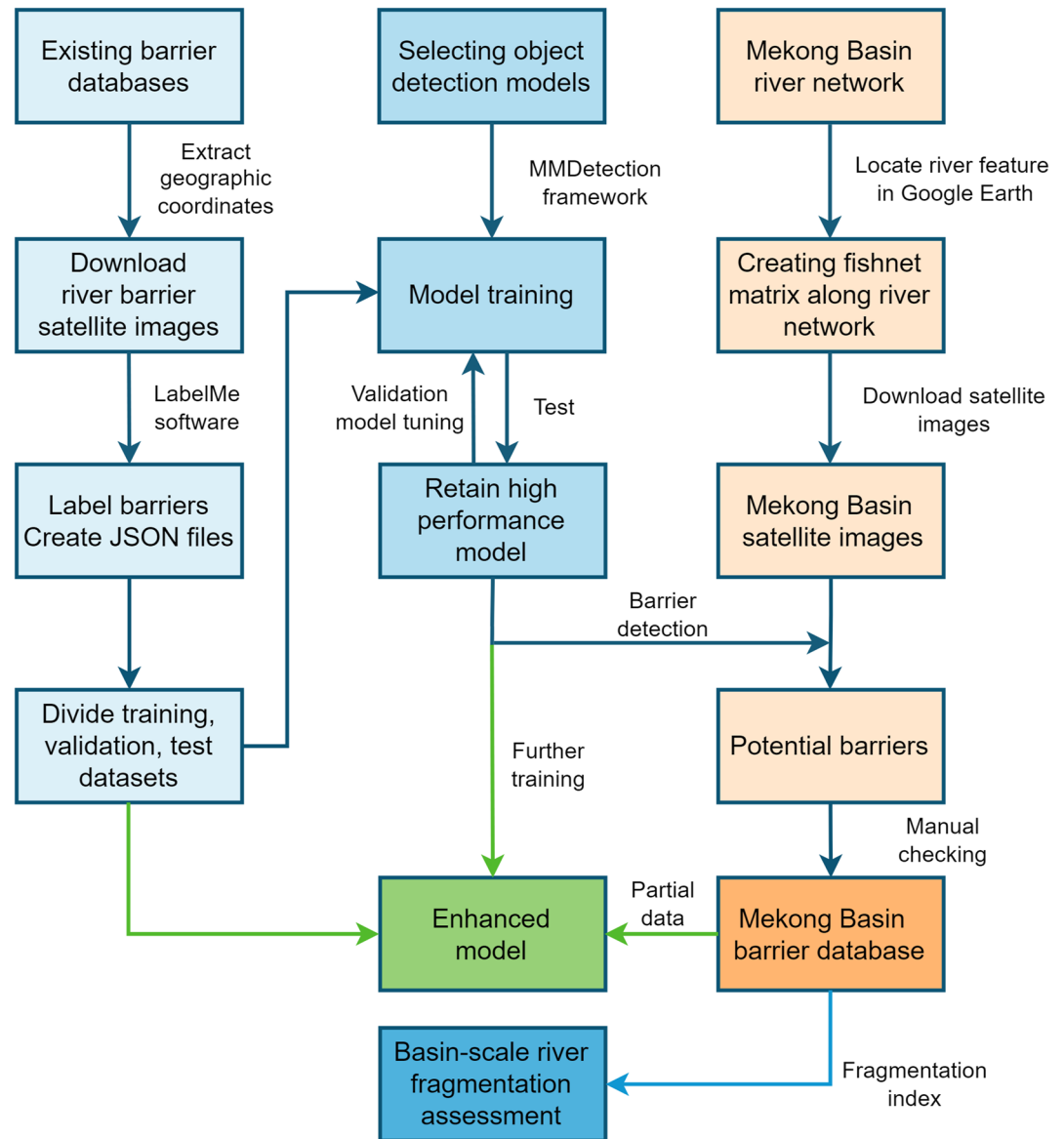


Figure 7. Flow chart of the model training and river fragmentation assessment process.

et al., 2022; Pebesma et al., 2022). Kruskal-Wallis H tests were used to compare the differences in median barrier densities between the three databases (GROD, GMSHD and MRBD), as well as barrier densities and CAFI values across the nine regions of the Mekong Basin. All statistical analysis were conducted in SPSS v25.

3. Results

3.1. Abundance and Distribution of River Barriers in the Mekong Basin

A total of 329,075 potential anthropogenic river barriers were identified in the Lower Mekong Basin by the CNN object detection model, when the score threshold exceeded 0.3. During the manual cleansing step, a total of 318,065 misidentified objects were removed and 11,010 river barriers were retained, comprising 7,827 dams, 883 weirs, 2,121 sluice gates, 46 bridge aprons, and 133 barriers of other types (e.g., heavily modified channel, cross channel fixed fishing gear). Then, an additional 854 manually detected barriers, including 633 dams (mostly [95.1%] consisting of simple earth dams), five weirs, 162 sluice gates, six bridge aprons, and 48 barriers of other types were added to the database. Furthermore, a total of 1.07 million images without barriers were correctly classified by the FCOS model.

Table 2
Comparison of Model Performance Between the Initial Retained Fully Convolutional One Stage (FCOS) Model and the Enhanced FCOS Model Across 20 Randomly Selected Sub-Basins in the Lower Mekong

Sub-basin	Region	Input satellite images	True positives		True negatives		Accuracy	
			Initial model	Enhanced model	Initial model	Enhanced model	Initial model	Enhanced model
1	HLR	3,527	14	21	3,354	3,385	95.5%	96.6%
2	HLR	2,788	28	46	2,521	2,538	91.4%	92.7%
3	HLR	10,027	17	26	9,747	9,841	97.4%	98.4%
4	HLR	1,777	26	54	1,228	1,426	70.6%	83.3%
5	MR	169	4	5	153	147	92.9%	89.9%
6	MR	4,014	2	16	3,741	3,877	93.2%	97.0%
7	MR	3,950	8	16	3,734	3,800	94.7%	96.6%
8	MR	1,303	14	35	1,155	1,169	89.7%	92.4%
9	MR	4,084	74	222	3,282	3,226	82.2%	84.4%
10	NNR	4,137	213	570	2,433	2,769	64.0%	80.7%
11	NNR	2,955	169	462	1,766	1,804	65.5%	76.7%
12	TSR	2,548	22	91	1,994	2,093	79.1%	85.7%
13	TSR	5,960	11	27	5,482	5,527	92.2%	93.2%
14	TSR	6,622	217	825	4,273	4,660	67.8%	82.8%
15	TSR	3,196	75	165	1,412	1,929	46.5%	65.5%
16	3S	3,658	30	33	3,348	3,352	92.3%	92.5%
17	3S	7,257	14	26	6,969	6,989	96.2%	96.7%
18	3S	7,152	110	345	6,113	5,718	87.0%	84.8%
19	ER	7,474	90	238	4,336	5,244	59.2%	73.3%
20	ER	3,247	13	29	1,943	2,249	60.2%	70.2%

Compared with river barriers identified by the initial FCOS model (recall = 0.935, $AP_{50} = 0.704$) and enhanced FCOS model (recall = 0.937, $AP_{50} = 0.752$) in 20 randomly selected Mekong sub-basins, the initial model was less efficient in the NNR and ER regions, due to relatively high numbers of simple earth dams and sluice gates missed, and misidentified objects such as field ridges. After more training data added, the performance of the enhanced model was substantially improved across all regions (Table 2), with an improved mean accuracy of 86.7% across these sub-basins compared with the initial model (mean accuracy = 80.9%).

Overall, a total of 11,864 barriers formed the Lower Mekong Barrier Database (LMBD). The LMBD was combined with the LRBD (Lancang River Barrier Database) to form the MRBD (Mekong River Barrier Database). After removing duplicates (the LRBD contained some barriers near the boundary of the UR and HLR regions that were duplicated in the LMBD) between the two barrier databases, a total of 13,054 river barriers including 8,795 dams, 1,689 weirs, 2,288 sluice gates, 101 bridge aprons, and 181 barriers of other types, belonging to 810 sub-basins, were recorded (Figure 8). In comparison, the existing database GROD recorded 123 dams and 60 weirs (111 dams and 55 weirs within the Lower Mekong Basin) belonging to 103 (89 within the Lower Mekong Basin) sub-basins, and the GMSHD recorded 398 dams (327 dams within the Lower Mekong Basin) belonging to 220 (189 within Lower Mekong) sub-basins (Figure S7 in Supporting Information S1). For the MRBD database, the NNR region contains the most river barriers ($n = 5,243$) as well as most dams ($n = 4,034$, mostly simple earth dams) and sluice gates ($n = 1,053$), followed by the MR region with 3,149 barriers including 2,458 dams; the HR1 and HR2 contain least barriers ($n = 73$ and 56 respectively). The CNN based method detected a total of 10,561 new barriers within the Lower Mekong Basin.

Across all six Mekong countries, Thailand has the most barriers across the Mekong Basin ($n = 8,187$) as well as most dams ($n = 6,484$) and sluice gates ($n = 1,398$) (Figure 8), followed by Vietnam with the second highest barrier numbers ($n = 1,389$) and sluice gate numbers ($n = 625$). China has a total of 1,302 Mekong barriers and

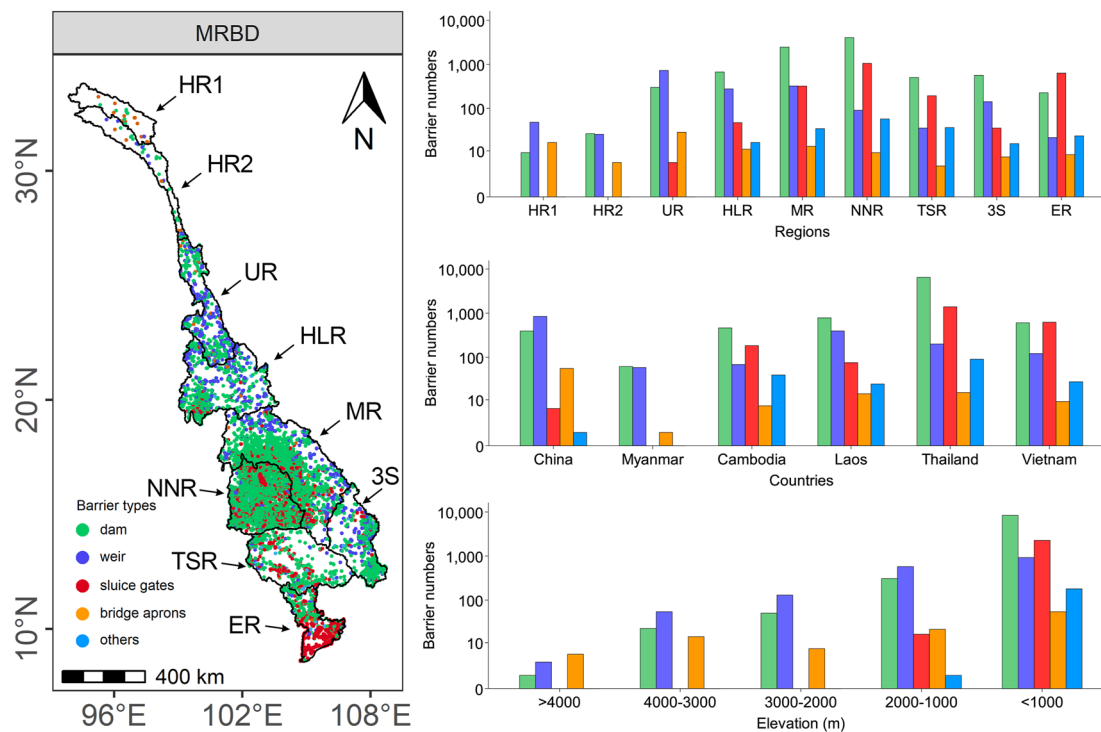


Figure 8. Distribution of anthropogenic river barrier types across the Mekong Basin. Left panel: locations of five types of barriers in the Mekong Basin recorded in the Mekong River Barrier Database; regions are indicated by arrowed abbreviations as in Figure 1. Right panel: distribution of five types of barriers in the Mekong Basin by regions (upper panel), countries (middle panel), and elevation (lower panel). Note the log y scale.

the most weirs ($n = 846$), followed by Laos ($n = 1,295$ total Mekong barriers), Cambodia ($n = 761$ total Mekong barriers), and Myanmar ($n = 120$ total Mekong barriers). Barriers were mostly distributed at elevations below 1,000 m, and barrier numbers steadily decreased with increased elevation, with only nine barriers above an elevation of 4,000 m (Figure 8).

3.2. River Fragmentation Level of the Mekong Basin

Across the Mekong Basin, the overall barrier density (median and [95% CI]) based on the MRBD database is 1.86 [0.00–25.41] per 100 km, significantly higher than barrier densities calculated from the GROD database (0.00 [0.00–0.57] per 100 km) and the GMSHD database (0.00 [0.00–1.01] per 100 km in both cases) (Kruskal-Wallis H test, $\chi^2(2) = 1,356$, $P < 0.001$). For the MRBD database, significant differences occurred in total barrier densities between regions (Figure 9, Kruskal-Wallis H test, $\chi^2(8) = 375.5$, $P < 0.001$). The NNR region has the highest total barrier density (15.53 [0.00–49.30] per 100 km), significantly higher than other regions (pairwise post hoc, $P < 0.001$ in all cases). The ER region has the second highest barrier density (5.07 [0.00–26.75] per 100 km), followed by the UR (2.86 [0.00–17.41] per 100 km) and MR (2.42 [0.00–18.23] per 100 km) regions. The most upstream HR1 and HR2 regions have the lowest barrier densities (0.00 [0.00–4.97] and 0.00 [0.00–1.92] per 100 km respectively).

Differences were found for dam densities across the nine regions (Figure 9, Kruskal-Wallis H test, $\chi^2(8) = 334.1$, $P < 0.001$, with the highest dam densities in the NNR region (11.66 [0.00–43.02] per 100 km) and lowest densities appeared in the HR1 and HR2 regions (0.00 [0.00–1.48] and 0.00 [0.00–1.45] per 100 km respectively). For weir densities, significant differences also occurred across regions (Figure 9, Kruskal-Wallis H test, $\chi^2(8) = 140.9$, $P < 0.001$), with the highest densities in the UR region (0.91 [0.00–15.30] per 100 km) and lowest densities in the HR1, HR2, and TSR regions. For sluice gates, densities in the NNR (3.01 [0.00–14.57] per 100 km) and ER (2.75 [0.00–21.28] per 100 km) regions were significantly higher compared with other regions (Kruskal-Wallis H test, $\chi^2(5) = 318.7$, $P < 0.001$; HR1, HR2, and UR regions were excluded from the analysis due to absent/very low numbers of sluice gates).

Use of a high (0.8) impassability coefficient resulted in higher median sub-basin Catchment Area-based Fragmentation Index than for a low (0.2) impassability coefficient ($P < 0.01$), but no difference with a moderate (0.5)

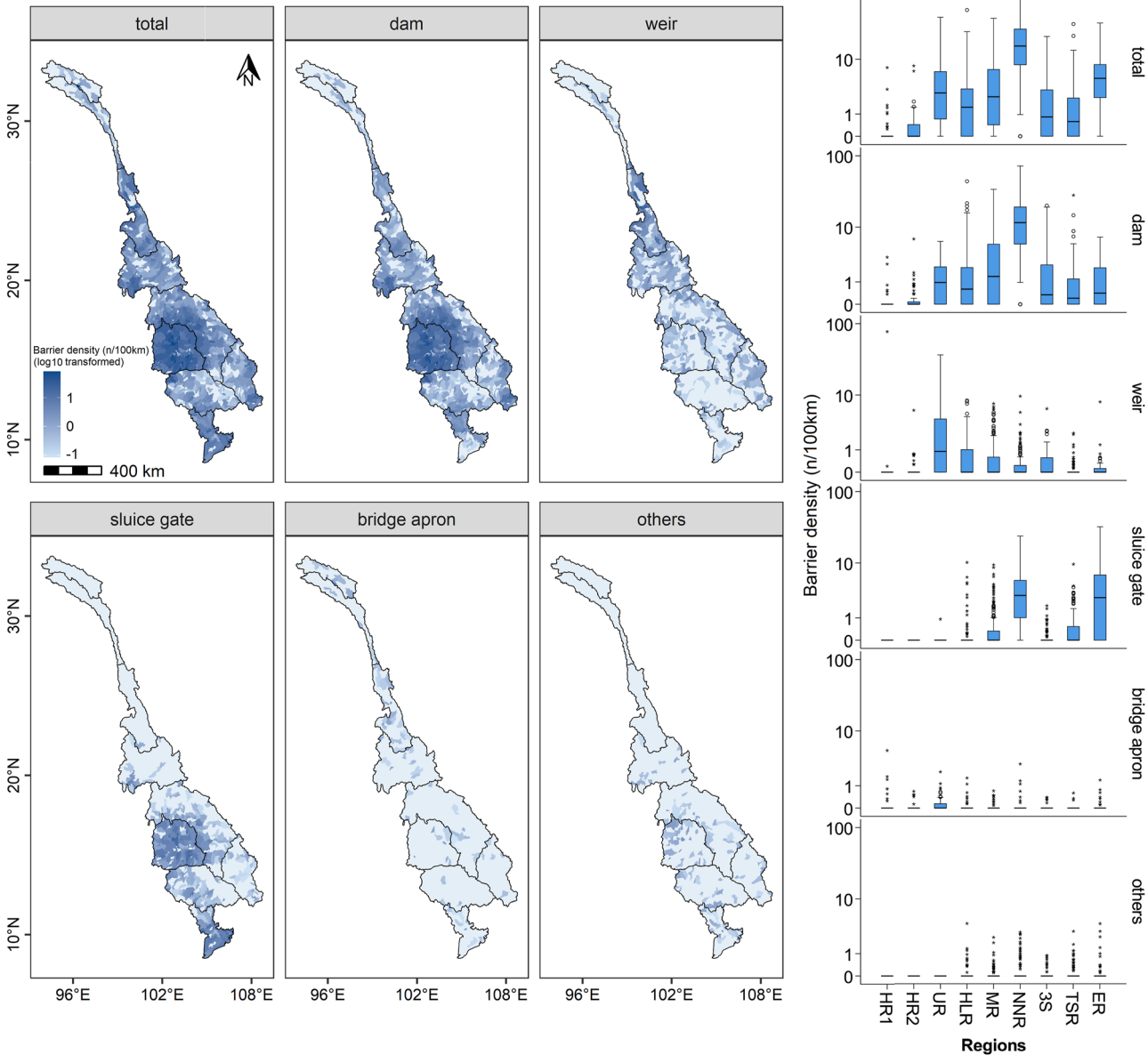


Figure 9. Regional distribution of anthropogenic river barrier types in the Mekong Basin. Left panel: Barrier densities (n/100 km) in each region of the Mekong Basin. Right panel: Box plots showing median (with quartiles, ranges, and outliers) barrier densities in each region of the Mekong Basin. Note the log scale. Full name of each region can be found in Figure 1.

impassability coefficient ($P > 0.05$, further detail in Supporting Information S1). Using an upstream-direction calculated CAFI index, with an impassability index of 0.5 for semi-permeable barriers (weirs, bridge aprons, sluice gates), and 1.0 for dams and other barriers, significant differences in median CAFI occurred between the nine Mekong regions (Figure 10, Kruskal-Wallis H test, $\chi^2(8) = 292.1$, $P < 0.001$). Median [95% CI] CAFI in the NNR region, 1,178.67 [0.00–6,418.46] (Figure 10), was significantly higher compared with other regions, followed by the ER region (455.35 [0.00–2,229.94]), and the lowest CAFI appeared in the HR1 (0.00 [0.00–255.13]) and HR2 regions (0.00 [0.00–280.68]).

4. Discussion

This study provides the first complete Mekong River barrier database covering five major types of anthropogenic river barriers, generated by the object detection approach combined with manual revision and merged with

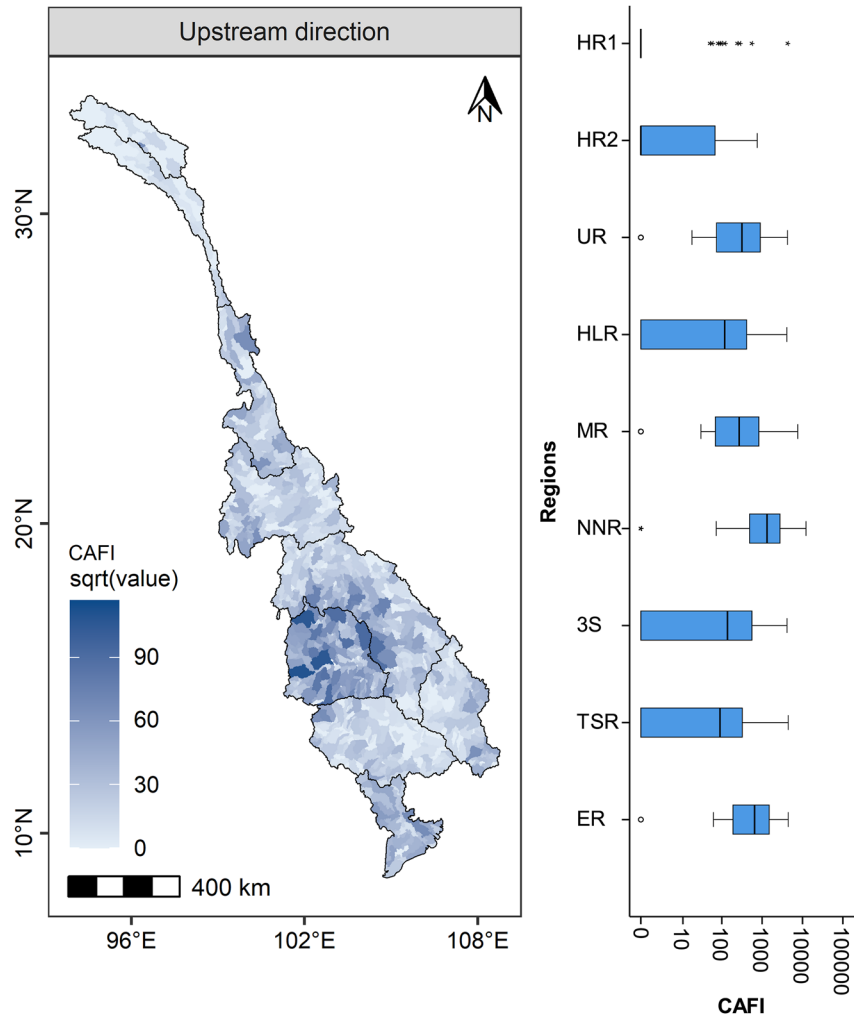


Figure 10. Catchment Area-based Fragmentation Index values across the Mekong Basin. Left panel: Catchment Area-based Fragmentation Index (CAFI) values at each region in the Mekong Basin. Impassability of 0.5 was assigned to weirs, bridge aprons and sluice gates, and 1.0 to dams and other barriers when calculating CAFI values here. Note the square root transformed scale. Right panel: box plots showing median (with quartiles, ranges, and outliers) CAFI in each region. Note the log scale.

the existing Lancang barrier database. We found that CNN-based object detection is effective in automatically identifying multiple types of river barrier, though a high frequency of commission errors occurred, necessitating manual revision. Nevertheless, our priority was the detection of previously unrecorded river barriers and this methodology enabled that in a way that would not have been possible by conventional barrier mapping methods. Across several models, the anchor-free one-stage method (FCOS ResNext-101-FPN) had better performance compared with multiple-stage methods. Furthermore, our study indicated that existing databases that covered the Lower Mekong are highly incomplete for the Lower Mekong Region, with 97%–99% of river barriers absent from the two existing databases (GROD, GMSHD). Furthermore, after adding 1,897 more images to the model, the accuracy of the enhanced FCOS model had increased from 80.9% to 86.7% compared to the initial model across the Lower Mekong Basin, reflecting a substantial improvement. Barrier densities calculated from the MRBD database were significantly higher compared with those calculated from existing databases, showing that previous assessments largely underestimated the true level of river fragmentation in the Lower Mekong.

4.1. Performance Comparisons Between Barrier Detection Models

The FCOS object detection approach captured more than 10,561 previously unrecorded river barriers in the Lower Mekong Basin (downstream of the Lancang), covering five different barrier types, suggesting it is a powerful tool

and can be applied to identify different river barriers in other large river basins with no, or limited, barrier information. Importantly, our trained model can be applied on freely accessed Google Earth satellite images or other open access remotely sensed images, and does not require acquisition of specialist remotely sensed data such as LIDAR and SAR. The barrier identification performances were better in anchor-free one-stage methods (FCOS and Foveabox) compared with anchor-based multi-stage methods. This is potentially due to the dataset used in training and validation containing large numbers of small-scale barriers. Detection of small objects has been a major challenge in object detection since it was developed (Pham et al., 2020; Tian et al., 2019). In anchor-based multi-stage methods, where the scales and aspect ratios of anchor boxes are kept fixed, detectors suffered difficulties in dealing with small-size candidates with large variations in shape (Tian et al., 2019). Even after tuning the anchor boxes, the recall rates of anchor-based multi-stage methods remained lower compared with anchor-free one-stage methods. The pre-defined anchor boxes also hamper the generalization ability of detectors, as they need to be re-designed for new detection tasks with different object sizes or aspect ratios. This is particularly the case for river barrier detection, due to the large variation in barrier sizes, in which the area of large-scale barriers, such as hydropower facilities or reservoir dams could be several magnitudes greater than small-scale barriers such as weirs, and even small-scale dams, in remotely sensed images (Figure 2).

4.2. Habitat Fragmentation Level of the Mekong Basin

Distribution of barriers across the Mekong Basin was found to be highly variable. In the most fragmented localities (i.e., the NNR region and western part of the MR region), high dam and sluice gate densities were related to the predominance of agricultural land use in Thailand, resulting in the construction of many simple earth dams, reservoir dams, and sluice gates to support farming and irrigation. In rural areas of Thailand, these irrigation systems have been widely applied for water resource management (Suntaranont et al., 2020). In addition, it was noticed that in this region many river channels, especially second- to fourth-order tributaries have suffered from heavy modification, and in some cases river channels were modified into multiple fragmented ponds or crop fields. This has resulted in these rivers having lost their function as free-flowing habitat for migratory aquatic species. Similarly, the ER region (i.e., the Mekong Delta) is one of the biggest rice producing regions in Asia, with the majority of its land area used for paddy rice farming by the Vietnamese government (Clauss et al., 2018). This has resulted in sluice gates and dams being increasingly built for protecting agricultural land from flooding, climate change -derived salinity intrusion, and supporting irrigation networks under increased cropping intensity (Hoanh et al., 2014). These barriers could pose significant threats to migratory fish species, especially those diadromous fishes that require free access between saltwater and freshwater habitat to complete their life cycle (Baumgartner et al., 2022; Sun et al., 2021).

For the UR region, high densities of weirs and small hydropower facilities are related to the rapid rural electrification in China (Bhattacharyya & Ohiare, 2012), and increased demand for irrigation water on crop fields (Gu et al., 2010). These small-scale barriers, and main channel cascade reservoirs have led to habitat loss for both locally resident and moderate-distance migratory fish species in the Upper Mekong region (Ding et al., 2023; Sun, Du, et al., 2023). For the 3S region, especially in the Vietnamese part, the construction of river barriers including hydropower dams is much more intensive compared with the Laos and Cambodia parts, which has resulted in the regional river connectivity and physical features being seriously affected (Bonnema et al., 2020; Shaad et al., 2018). The 3S region and the northern Cambodian Mekong River are considered to provide critical habitat for fish megafaunal species (Campbell et al., 2020). Although currently the main Mekong channel here is free from barrier construction, the Lower Sesan 2 Dam (commissioned in 2018) on the lower Sesan River has mostly blocked access to nearly two-thirds of critical habitat in the Sesan and Srepok Rivers for migratory fish species (Sun, Yu, et al., 2023). For other regions, although impacts of barrier construction on aquatic habitats were relatively low, concerns should be raised as even limited numbers of barriers could still pose significant threats to aquatic ecosystems (Sun et al., 2021, 2022; Zhang et al., 2019).

There is vigorous international debate concerning further river barrier development in the Mekong Basin and other large Asian transboundary rivers (Sun, Galib, et al., 2023; Tao, Bond, et al., 2023; Winemiller et al., 2016). This is particularly so for large hydropower in terms of the balance of costs and benefits to society and the environment, including the provision of key ecosystem services such as the fisheries that are vital in large parts of the lower Mekong Basin (Ziv et al., 2012). A further reason for the generation of a high-quality basin-wide inventory of small as well as large barriers is that, in attempting to mitigate the impacts of the building of large dams, an

alternative to building high-head bidirectional fish passes that, to date have often proved ineffectual in the tropics (Silva et al., 2018), is to provide improved passage at many small migration barriers in the locality (Baumgartner et al., 2022). This “offset” strategy of improving connectivity at weirs and road crossings on tributaries and at flood control sluices is more likely to be an economically effective means of supporting fisheries to compensate for the losses due to mainstream dams, but is reliant upon a relatively complete barrier database across subcatchments (Campbell & Barlow, 2020). During the visual interpretation in the 20 Lower Mekong sub-basins (during which we checked both 2020/21 and 2022/23 images), we recorded an addition of 16 newly constructed river barriers (majority constructed in the NNR and MR regions) since 2021, suggesting that barrier construction is still proceeding rapidly in Lower Mekong Basin countries. Ultimately a basin-wide barrier inventory is essential for planning aquatic habitat protection and connectivity for biodiverse freshwater fauna of the Mekong, including the charismatic megafish species (Campbell et al., 2020; Winemiller et al., 2016).

4.3. Limitations in Current Method and Potential Solutions

Potential limitations in this study deserve consideration. First, our barrier detection procedure requires both the object detection model and the manual revision step. The manual step is crucial for correcting commission and omission errors that occurred during the object detection process. For the Mekong Basin, the omission errors mostly occurred in Thailand (the NNR and western MR regions). Although the FCOS model outperformed other models when detecting small barriers, it still suffered difficulty in detecting certain types of small barriers such as simple earth dams and sluice gates. This is due to the fact that both types of barriers, in particular the simple earth dam, are endemic to South East Asia countries, especially Thailand, but are rarely constructed in other countries across the world. This resulted in these barriers being rarely recorded in existing databases, which limited their chance of being studied by the model. Furthermore, these small-scale barriers were generally constructed in low-order rivers, and their small size further increased the difficulty of being detected by the model. We manually surveyed over 23% of all images (that fraction in which the FCOS model identified potential barriers) to identify unrecorded barriers, especially earth dams, in order to reduce omission errors. After we added new data of simple earth dams and sluice gates to the training set, omission errors from the enhanced model were substantially (by 20.9%) reduced within these regions. To more fully solve this problem and reduce labor during the manual revision step in future, more images of these types of barriers need to be added to the training set in the future as an augmentation approach. For application of our method to other large river basins, the likelihood that enhanced training as described above, will be needed is dependent on the degree to which barrier types common to existing databases and available for CNN training, validation and testing are typical of those found in the basin to be investigated. If there is an unusual or atypical barrier type, not widely found in existing barrier dataset, as is the case for simple earth dams in flat, floodplain habitat for parts of the Lower Mekong, then enhanced training using many images of those barrier types will be needed.

Second, it was noticed that commission errors for the Mekong Basin were much more frequent compared with using the test set. During the manual cleansing step, we noticed that commission errors largely occurred in the ER region, with more than half of satellite images having generated false positives of artificial river barrier presence. Although enhanced model training reduced false positives to one third of the total images of the enhanced model, they remained highest within the ER region. As mentioned above, the majority of the land in this region has been converted into paddy rice fields. During the barrier detection process, considerable numbers of rice field ridges were wrongly identified as small dams or weirs, due to their similar physical features (water on both sides of the structure). In addition, small bridges (without barrier-forming bridge aprons) have been built in large numbers to support local traffic between rice fields, and many of these bridges were identified as small dams by the object detection model. Concerns should be raised when transferring our model to other basins with similar land features, and manual revision must be adopted associated with the object detection method to minimize commission errors. By contrast, along single thread river channels, where flooded field agriculture is rare (e.g., large parts of temperate Eurasia and North America) it is likely the CNN method developed here would work well, with much lower expected omission and commission errors. Similarly, to properly solve the commission error problem for the Mekong, more images within the ER region should be added to the current training set, to enhance the performance of the model. On the other hand, in the future, structures such as rice field ridges or bridges can potentially be labeled as separate classes during training, to enable the CNN model to autonomously distinguish them from genuine barriers. Also, spectral information (individual bands and their transformation) could be considered during the image processing stage, to further enhance the model performance.

Third, we generated the MRBD by combining the LRBD from Sun, Galib, et al. (2023) with the Lower Mekong barrier database generated here. The LRBD was solely obtained by visual searching and interpretation of barriers found in the Upper Mekong (Lancang), while the Lower Mekong barriers were generated mostly by CNN detection as potential barriers, confirmed by visual checking. Based on the analysis, visual searching was a more reliable but time consuming way of finding smaller barriers, especially earth dams and sluice gates. It is therefore likely that the Lancang Barrier database is more complete (in terms of percentage of the true number of barriers) than the Lower Mekong Barrier Database, but we do not anticipate this to markedly affect the utility of the overall database for conservation planning.

Lastly, although the model can detect visible barriers from satellite images, barriers that are obstructed from view, such as those covered by clouds, or located on small tributaries with dense tree canopies, cannot be seen from satellite images and therefore cannot be detected by the software. Similarly, some river barriers such as culverts at transport crossings cause negative effects on aquatic habitat and river connectivity (Januchowski-Hartley et al., 2013), but cannot be readily detected from satellite images due to their physical features (constructed underground). This probably results in certain types of barriers being missed from our database, which should be regarded as conservative in the extent of its inventory. Therefore, it is suggested that during future river barrier management actions, field-surveying should be combined with our database, to avoid missing barriers that are not apparent from satellite images, especially in urban or heavily tree-lined areas. Our next step would be to add the Lower Mekong Barrier Database (LMBD) to the satellite image database we created, and to train a new model to achieve better performance in detecting these small-scale river barriers, and apply it to other data-deficient large river basins (e.g., the Nu-Salween, Yuan-Red basins) for barrier collection. Furthermore, the effects of barrier construction on the habitat availability and river biodiversity in the Mekong Basin require full evaluation in future; publication of our open-access Mekong River Barrier Database will help enable this.

5. Conclusion

In this study, we proposed a new river barrier detection framework combined with a convolutional neural network-based object detection model combined with a manual revision step. Across several object detection models, the FCOS had better precision and recall compared with other multiple-stage methods. With this framework, we identified 10,561 previously unrecorded anthropogenic river barriers within satellite images for the Lower Mekong Basin, and assessed the habitat fragmentation level for the whole basin. It was found that the Mekong Thailand Region is the most fragmented locality, with highest earth dam and sluice gate densities, and highest CAFI values. The open-access Mekong River Barrier Database created in this study can provide baseline data to all Mekong countries, facilitate environmental protection and habitat restoration projects, and support management plans for future river connectivity restoration work. The new river barrier detection framework could be transferred to other data-deficient river basins for detecting both large- and small-scale river barriers.

Conflict of Interest

The authors declare no conflicts of interest relevant to this study.

Data Availability Statement

The barrier coordinates employed for creating the river barrier image training set are available in Belletti et al. (2020), Yang et al. (2022), and Sun, Du, et al. (2023). The trained FCOS model, R scripts, and the Mekong River Barrier Database generated in the study are available in Sun, Ding, et al. (2023).

References

- Atkinson, S., Bruen, M., Turner, J. N., Ball, B., Bullock, C., O'Sullivan, J. J., et al. (2018). The value of a desk study for building a national river obstacle inventory. *River Research and Applications*, 34(8), 1085–1094. <https://doi.org/10.1002/rra.3338>
- Barbarossa, V., Schmitt, R. J. P., Huijbregts, M. A. J., Zarfl, C., King, H., & Schipper, A. M. (2020). Impacts of current and future large dams on the geographic range connectivity of freshwater fish worldwide. *Proceedings of the National Academy of Sciences*, 117(7), 3648–3655. <https://doi.org/10.1073/pnas.1912776117>
- Baumgartner, L. J., Marsden, T., Duffy, D., Horta, A., & Ning, N. (2022). Optimizing efforts to restore aquatic ecosystem connectivity requires thinking beyond large dams. *Environmental Research Letters*, 17(1), 014008. <https://doi.org/10.1088/1748-9326/ac40b0>

Acknowledgments

The study was funded by the National Natural Science Foundation of China (42301064, 42077447), the China Postdoctoral Science Foundation (2021M702777), and the Yunnan Scientist Workstation on International River Research of Daming He (KXJGZS-2019-005). We thank Qi Liu, Chaoqing Zeng, Yongtao Zhao, Mengxue Zhang, Wenxin Liu, and Daomingyue Huang of the Institute of International Rivers and Eco-security, Yunnan University, for their assistance with river barrier verification.

- Belletti, B., Garcia de Leaniz, C., Jones, J., Bizzi, S., Börger, L., Segura, G., et al. (2020). More than one million barriers fragment Europe's rivers. *Nature*, 588(7838), 436–441. <https://doi.org/10.1038/s41586-020-3005-2>
- Bhattacharyya, S. C., & Ohiare, S. (2012). The Chinese electricity access model for rural electrification: Approach, experience and lessons for others. *Energy Policy*, 49, 676–687. <https://doi.org/10.1016/j.enpol.2012.07.003>
- Birnie-Gauvin, K., Candee, M. M., Baktoft, H., Larsen, M. H., Koed, A., & Aarestrup, K. (2018). River connectivity reestablished: Effects and implications of six weir removals on brown trout smolt migration. *River Research and Applications*, 34(6), 548–554. <https://doi.org/10.1002/rra.3271>
- Bivand, R., Keitt, T., Rowlingson, B., Pebesma, E., Sumner, M., Hijmans, R., et al. (2022). Package 'rgdal'. <https://cran.r-project.org/package=rgdal>
- Bivand, R., Rundel, C., Pebesma, E., Stuetz, R., Hufthammer, K. O., Giraudoux, P., et al. (2021). Package 'rgeos'. <https://cran.r-project.org/web/packages/rgeos/index.html>
- Bonnema, M., Hossain, F., Nijssen, B., & Holtgrieve, G. (2020). Hydropower's hidden transformation of rivers in the Mekong. *Environmental Research Letters*, 15(4), 044017. <https://doi.org/10.1088/1748-9326/ab763d>
- Buchanan, B. P., Sethi, S. A., Cuppett, S., Lung, M., Jackman, G., Zarr, L., et al. (2022). A machine learning approach to identify barriers in stream networks demonstrates high prevalence of unmapped riverine dams. *Journal of Environmental Management*, 302, 113952. <https://doi.org/10.1016/j.jenvman.2021.113952>
- Cai, Z., & Vasconcelos, N. (2019). Cascade R-CNN: High quality object detection and instance segmentation. *IEEE Transactions on Pattern Analysis and Machine Intelligence*, 43(5), 1483–1498. <https://doi.org/10.1109/tpami.2019.2956516>
- Campbell, I., & Barlow, C. (2020). Hydropower development and the loss of fisheries in the Mekong River basin. *Frontiers in Environmental Science*, 8, 566509. <https://doi.org/10.3389/fenvs.2020.566509>
- Campbell, T., Pin, K., Ngor, P., & Hogan, Z. (2020). Conserving Mekong megafishes: Current status and critical threats in Cambodia. *Water*, 12(6), 1820. <https://doi.org/10.3390/w12061820>
- Chen, K., Wang, J., Pang, J., Cao, Y., Xiong, Y., Li, X., et al. (2019). *MMDetection: Open MMLab detection toolbox and benchmark*. *arXiv preprint arXiv:1906.07155*.
- Clauss, K., Ottinger, M., Leinenkugel, P., & Kuenzer, C. (2018). Estimating rice production in the Mekong Delta, Vietnam, utilizing time series of Sentinel-1 SAR data. *International Journal of Applied Earth Observation and Geoinformation*, 73, 574–585. <https://doi.org/10.1016/j.jag.2018.07.022>
- Cote, D., Kehler, D. G., Bourne, C., & Wiersma, Y. F. (2009). A new measure of longitudinal connectivity for stream networks. *Landscape Ecology*, 24(1), 101–113. <https://doi.org/10.1007/s10980-008-9283-y>
- Couto, T. B. A., Messenger, M. L., & Olden, J. D. (2021). Safeguarding migratory fish via strategic planning of future small hydropower in Brazil. *Nature Sustainability*, 4(5), 409–416. <https://doi.org/10.1038/s41893-020-00665-4>
- Ding, C., Sun, J., Huang, M., Bond, N., Ding, L., & Tao, J. (2023). Flow and thermal regimes altered by a dam caused failure of fish recruitment in the upper Mekong River. *Freshwater Biology*, 68(8), 1319–1329. <https://doi.org/10.1111/fwb.14105>
- Entec (2010). *Mapping hydropower opportunities and sensitivities in England and Wales*. Technical Report, Environment Agency.
- Fang, W., Sun, Y., Ji, R., Wan, W., & Ma, L. (2021). Recognizing global dams from high-resolution remotely sensed images using convolutional neural networks. *Ieee Journal of Selected Topics in Applied Earth Observations and Remote Sensing*, 14, 6363–6371. <https://doi.org/10.1109/JSTARS.2021.3088520>
- Fang, W., Wang, C., Chen, X., Wan, W., Li, H., Zhu, S., et al. (2019). Recognizing global reservoirs from Landsat 8 images: A deep learning approach. *IEEE Journal of Selected Topics in Applied Earth Observations and Remote Sensing*, 12(9), 3168–3177. <https://doi.org/10.1109/JSTARS.2019.2929601>
- Garcia de Leaniz, C., & O'Hanley, J. R. (2022). Operational methods for prioritizing the removal of river barriers: Synthesis and guidance. *Science of the Total Environment*, 848, 157471. <https://doi.org/10.1016/j.scitotenv.2022.157471>
- Grill, G., Lehner, B., Thieme, M., Geenen, B., Tickner, D., Antonelli, F., et al. (2019). Mapping the world's free-flowing rivers. *Nature*, 569(7755), 215–221. <https://doi.org/10.1038/s41586-019-1111-9>
- Grill, G., Ouellet Dallaire, C., Fluet Chouinard, E., Sindorf, N., & Lehner, B. (2014). Development of new indicators to evaluate river fragmentation and flow regulation at large scales: A case study for the Mekong River basin. *Ecological Indicators*, 45, 148–159. <https://doi.org/10.1016/j.ecolind.2014.03.026>
- Gu, S., He, D., Cui, Y., & Li, Y. (2010). Variations of agricultural water requirements in Lancang River basin in last 50 years. *Acta Geographica Sinica*, 65(11), 1355–1362.
- Hijmans, R. J., Bivand, R., Forner, K., Ooms, J., Pebesma, E., & Sumner, M. D. (2022). Package 'terra'. <https://cran.r-project.org/web/packages/terra/terra.pdf>
- Hoanh, C. T., Suhardiman, D., & Anh, L. T. (2014). Irrigation development in the Vietnamese Mekong Delta: Towards polycentric water governance? *International Journal of Water Governance*, 2(2), 61–82. <https://doi.org/10.7564/14-IJWG59>
- Hung, N. N., Delgado, J. M., Tri, V. K., Hung, L. M., Merz, B., Bárdossy, A., & Apel, H. (2012). Floodplain hydrology of the Mekong delta, Vietnam. *Hydrological Processes*, 26(5), 674–686. <https://doi.org/10.1002/hyp.8183>
- Januchowski-Hartley, S. R., McIntyre, P. B., Diebel, M., Doran, P. J., Infante, D. M., Joseph, C., & Allan, J. D. (2013). Restoring aquatic ecosystem connectivity requires expanding inventories of both dams and road crossings. *Frontiers in Ecology and the Environment*, 11(4), 211–217. <https://doi.org/10.1890/120168>
- Jing, M., Cheng, L., Ji, C., Mao, J., Li, N., Duan, Z., et al. (2021). Detecting unknown dams from high-resolution remote sensing images: A deep learning and spatial analysis approach. *International Journal of Applied Earth Observation and Geoinformation*, 104, 102576. <https://doi.org/10.1016/j.jag.2021.102576>
- Jones, J., Börger, L., Tummers, J., Jones, P., Lucas, M., Kerr, J., et al. (2019). A comprehensive assessment of stream fragmentation in Great Britain. *Science of the Total Environment*, 673, 756–762. <https://doi.org/10.1016/j.scitotenv.2019.04.125>
- Jones, P. E., Champneys, T., Vevers, J., Börger, L., Svendsen, J. C., Consuegra, S., et al. (2021). Selective effects of small barriers on river-resident fish. *Journal of Applied Ecology*, 58(7), 1487–1498. <https://doi.org/10.1111/1365-2664.13875>
- Jumani, S., Deitch, M. J., Kaplan, D., Anderson, E. P., Krishnaswamy, J., Lecours, V., & Whiles, M. R. (2020). River fragmentation and flow alteration metrics: A review of methods and directions for future research. *Environmental Research Letters*, 15(12), 123009. <https://doi.org/10.1088/1748-9326/abcb37>
- Jumani, S., Deitch, M. J., Valle, D., Machado, S., Lecours, V., Kaplan, D., et al. (2022). A new index to quantify longitudinal river fragmentation: Conservation and management implications. *Ecological Indicators*, 136, 108680. <https://doi.org/10.1016/j.ecolind.2022.108680>
- Kang, B., & Huang, X. (2021). Mekong fishes: Biogeography, migration, resources, threats, and conservation. *Reviews in Fisheries Science & Aquaculture*, 30(2), 1–38. <https://doi.org/10.1080/23308249.2021.1906843>

- King, S., O'Hanley, J. R., Newbold, L. R., Kemp, P. S., & Diebel, M. W. (2017). A toolkit for optimizing fish passage barrier mitigation actions. *Journal of Applied Ecology*, 54(2), 599–611. <https://doi.org/10.1111/1365-2664.12706>
- Kong, T., Sun, F., Liu, H., Jiang, Y., Li, L., & Shi, J. (2020). Foveabox: Beyond anchor-based object detection. *IEEE Transactions on Image Processing*, 29, 7389–7398. <https://doi.org/10.1109/tip.2020.3002345>
- Lehner, B., Liermann, C. R., Revenga, C., Vörösmarty, C., Fekete, B., Crouzet, P., et al. (2011). High-resolution mapping of the world's reservoirs and dams for sustainable river-flow management. *Frontiers in Ecology and the Environment*, 9(9), 494–502. <https://doi.org/10.1890/100125>
- Lin, T. Y., Maire, M., Belongie, S., Hays, J., Perona, P., Ramanan, D., et al. (2014). Microsoft coco: Common objects in context. In *Computer Vision—ECCV 2014: 13th European Conference, Zurich, Switzerland, September 6–12, 2014, Part V 13* (pp. 740–755). Springer International Publishing.
- Liu, X., Han, F., Ghazali, K. H., Mohamed, I. I., & Zhao, Y. (2019). A review of convolutional neural networks in remote sensing image. *Proceedings of the 2019 8th International Conference on Software and Computer Applications*, 263–267. <https://doi.org/10.1145/3316615.3316712>
- Lucas, M. C., & Baras, E. (2001). *Migration of freshwater fishes*. Blackwell Science, Oxford.
- Lucas, M. C., Bubb, D. H., Jang, M.-H., Ha, K., & Masters, J. E. G. (2009). Availability of and access to critical habitats in regulated rivers: Effects of low-head barriers on threatened lampreys. *Freshwater Biology*, 54(3), 621–634. <https://doi.org/10.1111/j.1365-2427.2008.02136.x>
- Moortgat, J., Li, Z., Durand, M., Howat, I., Yadav, B., & Dai, C. (2022). Deep learning models for river classification at sub-meter resolutions from multispectral and panchromatic commercial satellite imagery. *Remote Sensing of Environment*, 282, 113279. <https://doi.org/10.1016/j.rse.2022.113279>
- Open Development Mekong (2016). Greater Mekong subregion hydropower dams. Retrieved from <https://data.opendevlopmentmekong.net/dataset/greater-mekong-subregion-hydropower-dams-2016>
- Pang, J., Chen, K., Shi, J., Feng, H., Ouyang, W., & Lin, D. (2019). Libra R-CNN: Towards balanced learning for object detection. *Proceedings of the IEEE/CVF conference on computer vision and pattern recognition* (pp. 821–830).
- Pebesma, E., Bivand, R., Racine, E., Sumner, M., Cook, I., Keitt, T., et al. (2022). Package 'sf'. <https://cran.r-project.org/web/packages/sf/index.html>
- Pham, M.-T., Courtrai, L., Friguet, C., Lefèvre, S., & Baussard, A. (2020). YOLO-Fine: One-Stage detector of small objects under various backgrounds in remote sensing images. *Remote Sensing*, 12(15), 2501. <https://doi.org/10.3390/rs12152501>
- Poff, N. L., Allan, J. D., Bain, M. B., Karr, J. R., Prestegard, K. L., Richter, B. D., et al. (1997). The natural flow regime. *BioScience*, 47(11), 769–784. <https://doi.org/10.2307/1313099>
- Radinger, J., Hölker, F., Horký, P., Slavík, O., & Wolter, C. (2018). Improved river continuity facilitates fishes' abilities to track future environmental changes. *Journal of Environmental Management*, 208, 169–179. <https://doi.org/10.1016/j.jenvman.2017.12.011>
- Reid, A. J., Carlson, A. K., Creed, I. F., Eliason, E. J., Gell, P. A., Johnson, P. T. J., et al. (2019). Emerging threats and persistent conservation challenges for freshwater biodiversity. *Biological Reviews*, 94(3), 849–873. <https://doi.org/10.1111/brv.12480>
- Ren, S., He, K., Girshick, R., & Sun, J. (2015). Faster R-CNN: Towards real-time object detection with region proposal networks. *Advances in Neural Information Processing Systems*, 28.
- Rodeles, A. A., Galicia, D., & Miranda, R. (2021). A simple method to assess the fragmentation of freshwater fish meta-populations: Implications for river management and conservation. *Ecological Indicators*, 125, 107557. <https://doi.org/10.1016/j.ecolind.2021.107557>
- Rouault, E., Taves, M., & Slave, M. (2021). GDAL/OGRE Geospatial data abstraction software library. Retrieved from <https://gdal.org/>
- Russell, B. C., Torralba, A., Murphy, K. P., & Freeman, W. T. (2008). LabelMe: A database and web-based tool for image annotation. *International Journal of Computer Vision*, 77(1–3), 157–173. <https://doi.org/10.1007/s11263-007-0090-8>
- Saeed, F., Ahmed, M. J., Gul, M. J., Hong, K. J., Paul, A., & Kavitha, M. S. (2021). A robust approach for industrial small-object detection using an improved faster regional convolutional neural network. *Scientific Reports*, 11(1), 23390. <https://doi.org/10.1038/s41598-021-02805-y>
- Segal-Rozenhaimer, M., Li, A., Das, K., & Chirayath, V. (2020). Cloud detection algorithm for multi-modal satellite imagery using convolutional neural networks (CNN). *Remote Sensing of Environment*, 237, 111446. <https://doi.org/10.1016/j.rse.2019.111446>
- Shaad, K., Souter, N. J., Farrell, T., Vollmer, D., & Regan, H. M. (2018). Evaluating the sensitivity of dendritic connectivity to fish pass efficiency for the Sesan, Srepok and Sekong tributaries of the Lower Mekong. *Ecological Indicators*, 91, 570–574. <https://doi.org/10.1016/j.ecolind.2018.04.034>
- Silva, A. T., Lucas, M. C., Castro-Santos, T., Katopodis, C., Baumgartner, L. J., Thiem, J. D., et al. (2018). The future of fish passage science, engineering, and practice. *Fish and Fisheries*, 19(2), 340–362. <https://doi.org/10.1111/faf.12258>
- Sofi, M. S., Bhat, S. U., Rashid, I., & Kuniyal, J. C. (2020). The natural flow regime: A master variable for maintaining river ecosystem health. *Ecology*, 13(8), e2247. <https://doi.org/10.1002/eco.2247>
- Spinti, R. A., Condon, L. E., & Zhang, J. (2023). The evolution of dam induced river fragmentation in the United States. *Nature Communications*, 14(1), 3820. <https://doi.org/10.1038/s41467-023-39194-x>
- Sun, J., Ding, C., Lucas, M. C., Tao, J., Cheng, H., Chen, J., et al. (2023). Data archive for 'Convolutional neural networks facilitate river barrier detection and evidence severe habitat fragmentation in the Mekong River biodiversity hotspot. [Dataset]. <https://zenodo.org/records/10141668>
- Sun, J., Du, W., Lucas, M. C., Ding, C., Chen, J., Tao, J., & He, D. (2023). River fragmentation and barrier impacts on fishes have been greatly underestimated in the Upper Mekong River. *Journal of Environmental Management*, 327, 116817. <https://doi.org/10.1016/j.jenvman.2022.116817>
- Sun, J., Galib, S. M., & Lucas, M. C. (2020). Are national barrier inventories fit for stream connectivity restoration needs? A test of two catchments. *Water and Environment Journal*, 34(S1), 791–803. <https://doi.org/10.1111/wej.12578>
- Sun, J., Galib, S. M., & Lucas, M. C. (2021). Rapid response of fish and aquatic habitat to removal of a tidal barrier. *Aquatic Conservation: Marine and Freshwater Ecosystems*, 31(7), 1802–1816. <https://doi.org/10.1002/aqc.3576>
- Sun, J., Galib, S. M., Ding, L., Tao, J., Ding, C., & He, D. (2023). Research status of the Lancang-Mekong river basin: Fish and environmental stressors. *Reviews in Fish Biology and Fisheries*, 33, 89–109. <https://doi.org/10.1007/s11160-022-09740-9>
- Sun, J., Tummers, J. S., Galib, S. M., & Lucas, M. C. (2022). Fish community and abundance response to improved connectivity and more natural hydromorphology in a post-industrial subcatchment. *Science of the Total Environment*, 802, 149720. <https://doi.org/10.1016/j.scitotenv.2021.149720>
- Sun, J., Yu, F., Zhang, Q., Luo, S., Zhou, W., Zhang, H., et al. (2023). Evaluation of a Nature-like Bypass for Non-Salmonids in the Sesan River. *Water*, 15(3), 421. <https://doi.org/10.3390/w15030421>
- Suntaranont, B., Aramkul, S., Kaewmoracharoen, M., & Champrasert, P. (2020). Water irrigation decision support system for practical weir adjustment using artificial intelligence and machine learning techniques. *Sustainability*, 12(5), 1763. <https://doi.org/10.3390/su12051763>
- Tao, J., Bond, N., Tun, N. N., & Ding, C. (2023). Keep the Salween River free-flowing. *Science*, 381(6656), 383–384. <https://doi.org/10.1126/science.ad9117>
- Tao, J., Ding, C., Chen, J., Ding, L., Brosse, S., Heino, J., et al. (2023). Boosting freshwater fish conservation with high-resolution distribution mapping across a large territory. *Conservation Biology*, 37(3), e14036. <https://doi.org/10.1111/cobi.14036>

- Tian, Z., Shen, C., Chen, H., & He, T. (2019). FCOS: Fully convolutional one-stage object detection. *Proceedings of the IEEE/CVF international conference on computer vision*, 9627–9636. <https://doi.org/10.48550/arXiv.1904.01355>
- Vörösmarty, C. J., McIntyre, P. B., Gessner, M. O., Dudgeon, D., Prusevich, A., Green, P., et al. (2010). Global threats to human water security and river biodiversity. *Nature*, *467*(7315), 555–561. <https://doi.org/10.1038/nature09440>
- Wang, Z., Liu, J., Li, J., Meng, Y., Pokhrel, Y., & Zhang, H. (2021). Basin-scale high-resolution extraction of drainage networks using 10-m Sentinel-2 imagery. *Remote Sensing of Environment*, *255*, 112281. <https://doi.org/10.1016/j.rse.2020.112281>
- Winemiller, K. O., McIntyre, P. B., Castello, L., Fluet-Chouinard, E., Giarrizzo, T., Nam, S., et al. (2016). Balancing hydropower and biodiversity in the Amazon, Congo and Mekong. *Science*, *351*(6269), 128–129. <https://doi.org/10.1126/science.aac7082>
- Wohl, E. (2017). Connectivity in rivers. *Progress in Physical Geography: Earth and Environment*, *41*(3), 345–362. <https://doi.org/10.1177/0309133317714972>
- Yang, X., Pavelsky, T. M., Ross, M. R. v., Januchowski-Hartley, S. R., Dolan, W., Altenau, E. H., et al. (2022). Mapping flow-obstructing structures on global rivers. *Water Resources Research*, *58*(1). <https://doi.org/10.1029/2021WR030386>
- Zhang, C., Ding, C., Ding, L., Chen, L., Hu, J., Tao, J., & Jiang, X. (2019). Large-scale cascaded dam constructions drive taxonomic and phylogenetic differentiation of fish fauna in the Lancang River, China. *Reviews in Fish Biology and Fisheries*, *29*(4), 895–916. <https://doi.org/10.1007/s11160-019-09580-0>
- Ziv, G., Baran, E., Nam, S., Rodriguez-Iturbe, I., & Levin, S. (2012). Trading-off fish biodiversity, food security, and hydropower in the Mekong River basin. *Proceedings of the National Academy of Sciences of the U.S.A.*, *109*(15), 5609–5614. <https://doi.org/10.1073/pnas.1201423109>